

## Supporting Information for

### Anion-dependent dysprosium (III) cluster single-molecule magnets

Cai-Ming Liu,\* and Xiang Hao

*Beijing National Laboratory for Molecular Sciences, CAS Key Laboratory for Organic Solids, Institute of Chemistry, Chinese Academy of Sciences, Beijing 100190, China. E-mail: cmliu@iccas.ac.cn.*

1. Figs S1-S3. IR spectra of H<sub>2</sub>L, **1** and **2**.
2. Table S1. Crystal Data and Structural Refinement Parameters for **1** and **2**.
3. Tables S2 and S3. Dy (III) ion geometry analysis by SHAPE 2.1 software for **1** and **2**.
4. Figs S4 and S5. *M versus H* plots at 2-6 K of **1** and **2**.
5. Table S4. Linear combination of two modified Debye model fitting parameters from 3 K to 14 K of **1** at 0 Oe dc field.
6. Fig. S6. Plots of  $\chi''$  versus *T* for **1** ( $H_{dc} = 1500$  Oe).
7. Fig. S7. Plots of  $\chi''$  versus  $\nu$  for **1** ( $H_{dc} = 1500$  Oe).
8. Fig. S8. Plot of  $\ln(\tau)$  versus  $1/T$  for **1** ( $H_{dc} = 1500$  Oe).
9. Fig. S9. Hysteresis loop for **1** at 1.9 K.
10. Table S5. Linear combination of two modified Debye model fitting parameters from 4 K to 17 K of **2** at 0 Oe dc field.
11. Fig. S10. Plots of  $\chi''$  versus *T* for **2** ( $H_{dc} = 1500$  Oe).
12. Fig. S11. Plots of  $\chi''$  versus  $\nu$  for **2** ( $H_{dc} = 1500$  Oe).
13. Fig. S12. Plot of  $\ln(\tau)$  versus  $1/T$  for **2** ( $H_{dc} = 1500$  Oe).
14. Fig. S13. Hysteresis loop for **2** at 1.9 K.

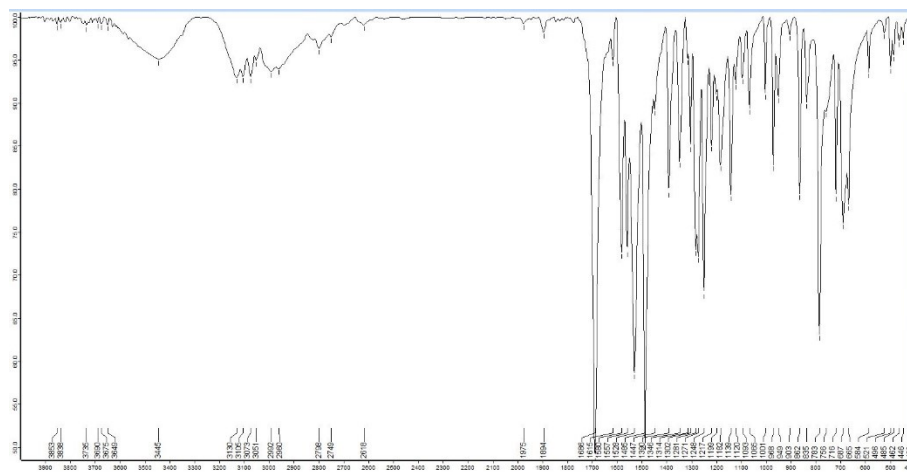


**Fig. S1.** IR spectrum of H<sub>2</sub>L.

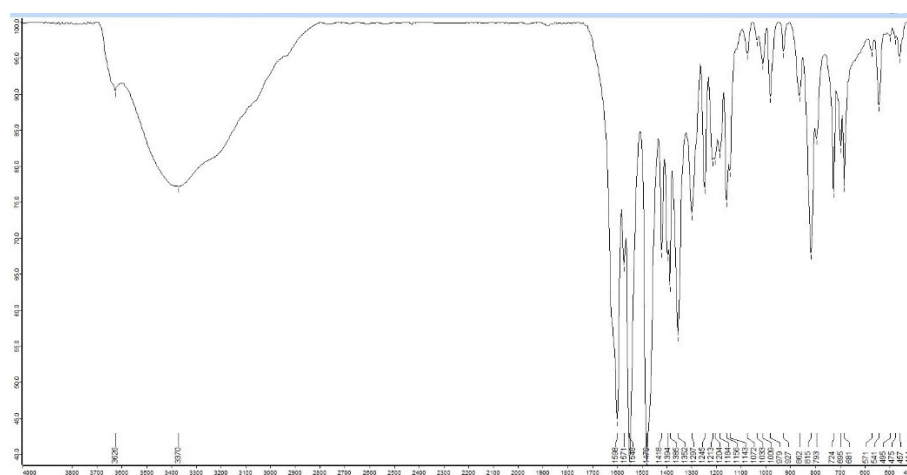


**Fig. S2.** IR spectrum of 1.

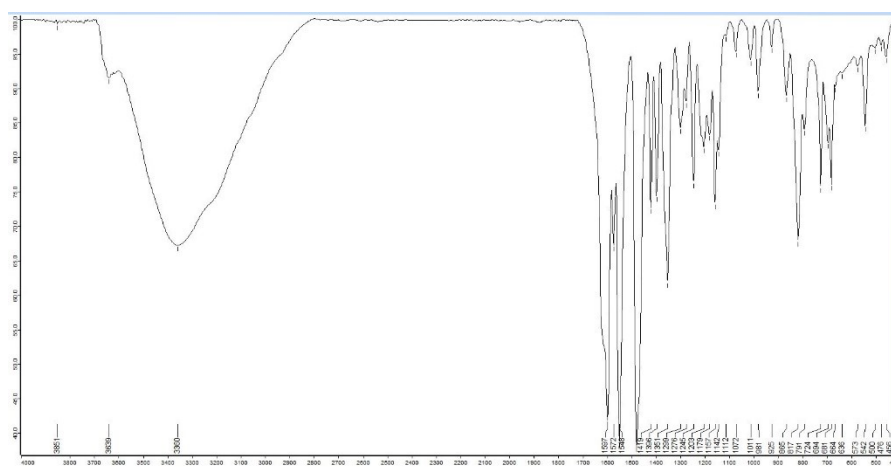


**Fig. S3.** IR spectrum of 2.

**Table S1.** Crystal Data and Structural Refinement Parameters for **1** and **2**.

	<b>1</b>	<b>2</b>
formula	C <sub>57</sub> H <sub>56</sub> Dy <sub>4</sub> F <sub>4</sub> N <sub>22</sub> O <sub>20</sub>	C <sub>80</sub> H <sub>71</sub> Cl <sub>2</sub> Dy <sub>6</sub> F <sub>6</sub> N <sub>24</sub> O <sub>27</sub>
$F_w$	2095.23	2960.50
crystal system	triclinic	monoclinic
space group	<i>P</i> -1	<i>P</i> 2 <sub>1</sub> / <i>n</i>
$a$ [Å]	12.74600(10)	14.2124(2)
$b$ [Å]	13.98880(10)	26.5826(4)
$c$ [Å]	20.3905(2)	26.3977(5)
$\alpha$ [°]	75.6740(10)	90.00
$\beta$ [°]	80.4120(10)	101.5751(17)
$\gamma$ [°]	86.0850(10)	90.00
$V$ [Å <sup>3</sup> ]	3472.00(5)	9770.3(3)
$Z$	2	4
$\rho_{\text{calc}}$ [g · cm <sup>-3</sup> ]	2.004	2.013
$\mu$ [mm <sup>-1</sup> ]	4.354	4.683
$T$ [K]	170	170
$\lambda$ (Mo-K $\alpha$ )[Å]	0.71073	0.71073
reflections collected	89284	147127
unique reflections	12281	22402
observed reflections	11779	18558
parameters	989	1424
GoF	1.040	1.098
$R_1$	0.0207	0.0794
$wR_2$	0.0544	0.2064
CCDC	2283183	2283184

**Table S2.** Dy (III) ion geometry analysis by SHAPE 2.1 software for **1**.

Configuration	ABOXIY <b>Dy1</b>	Configuration	ABOXIY <b>Dy2</b>	ABOXIY <b>Dy3</b>	ABOXIY <b>Dy4</b>
Octagon( $D_{8h}$ )	31.811	Enneagon( $D_{9h}$ )	33.390	32.430	35.582
Heptagonal pyramid( $C_{7v}$ )	24.409	Octagonal pyramid( $C_{8v}$ )	21.061	23.472	23.368
Cube ( $O_h$ )	14.653	Heptagonal bipyramid( $D_{7h}$ )	16.847	18.701	16.287
Hexagonal bipyramid( $D_{6h}$ )	13.545	Johnson triangular cupola J3( $C_{3v}$ )	13.833	14.004	15.070
Square antiprism ( $D_{4d}$ )	3.717	Capped cube J8( $C_{4v}$ )	9.496	10.517	9.479
Triangular dodecahedron ( $D_{2d}$ )	<b>1.547</b>	Spherical-relaxed capped cube( $C_{4v}$ )	7.935	9.524	8.236
Johnson gyrobifastigium J26 ( $D_{2d}$ )	11.392	Capped square antiprism J10( $C_{4v}$ )	2.758	2.812	2.063
Johnson elongated triangular bipyramid J14 ( $D_{3h}$ )	28.388	Spherical capped square antiprism( $C_{4v}$ )	<b>1.617</b>	1.989	<b>1.039</b>
Biaugmented trigonal prism J50 ( $C_{2v}$ )	3.524	Tricapped trigonal prism J51( $D_{3h}$ )	2.805	2.798	3.256
Biaugmented trigonal prism ( $C_{2v}$ )	2.642	Spherical tricapped trigonal prism( $D_{3h}$ )	2.091	2.708	2.165
Snub diphenoid J84 ( $D_{2d}$ )	3.509	Tridiminished icosahedron J63( $C_{3v}$ )	12.148	12.078	11.806
Triakis tetrahedron ( $T_d$ )	14.028	Hula-hoop( $C_{2v}$ )	12.077	9.456	11.445
Elongated trigonal bipyramid ( $D_{3h}$ )	23.937	Muffin( $C_s$ )	1.927	<b>1.672</b>	1.538

**Table S3.** Dy (III) ion geometry analysis by SHAPE 2.1 software for **2**.

Configuration	ABOXIY <b>Dy1</b>	ABOXIY <b>Dy2</b>	ABOXIY <b>Dy3</b>	ABOXIY <b>Dy4</b>	ABOXIY <b>Dy5</b>	ABOXIY <b>Dy6</b>
Octagon( $D_{8h}$ )	31.267	31.777	31.632	32.797	32.037	31.212
Heptagonal pyramid( $C_{7v}$ )	22.446	22.451	22.289	21.776	22.277	22.444
Hexagonal bipyramid( $D_{6h}$ )	16.688	16.120	16.662	16.436	16.899	15.608
Cube ( $O_h$ )	14.447	13.365	13.017	14.147	13.418	11.917
Square antiprism ( $D_{4d}$ )	4.468	4.054	3.887	4.862	3.913	4.058
Triangular dodecahedron ( $D_{2d}$ )	3.422	3.247	<b>2.654</b>	3.065	3.003	<b>2.983</b>
Johnson gyrobifastigium J26 ( $D_{2d}$ )	13.168	14.226	13.546	12.964	14.017	13.980
Johnson elongated triangular bipyramid J14 ( $D_{3h}$ )	25.046	27.521	26.917	24.194	26.500	27.379
Biaugmented trigonal prism J50 ( $C_{2v}$ )	2.852	3.468	2.737	<b>3.008</b>	<b>2.801</b>	3.665
Biaugmented trigonal prism ( $C_{2v}$ )	<b>2.728</b>	<b>3.240</b>	2.807	3.089	2.826	3.336
Snub diphenoid J84 ( $D_{2d}$ )	4.723	5.092	4.235	4.575	4.637	5.169
Triakis tetrahedron ( $T_d$ )	14.800	14.021	13.380	14.443	13.896	12.686
Elongated trigonal bipyramid ( $D_{3h}$ )	22.888	24.276	23.949	22.396	23.987	23.671

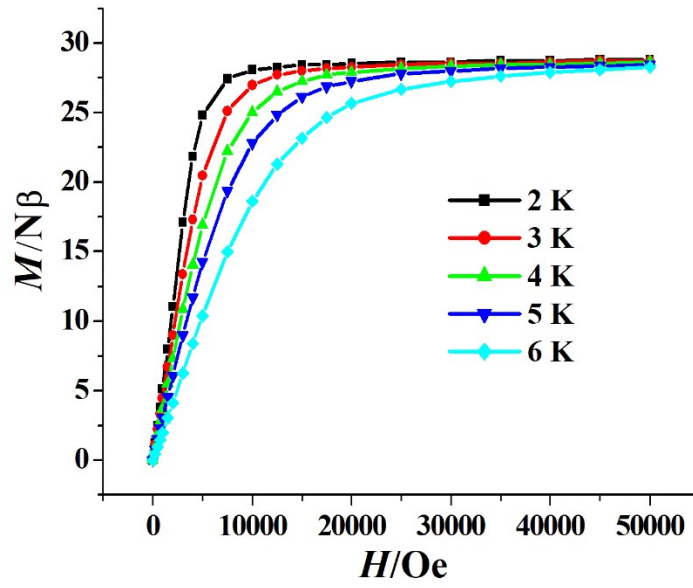


Fig. S4.  $M$  versus  $H$  plots at 2-6 K of 1.

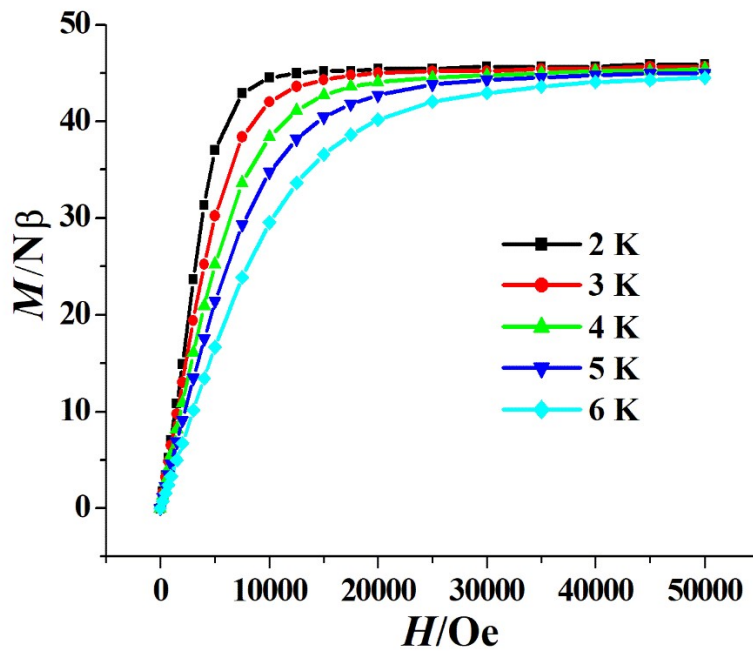
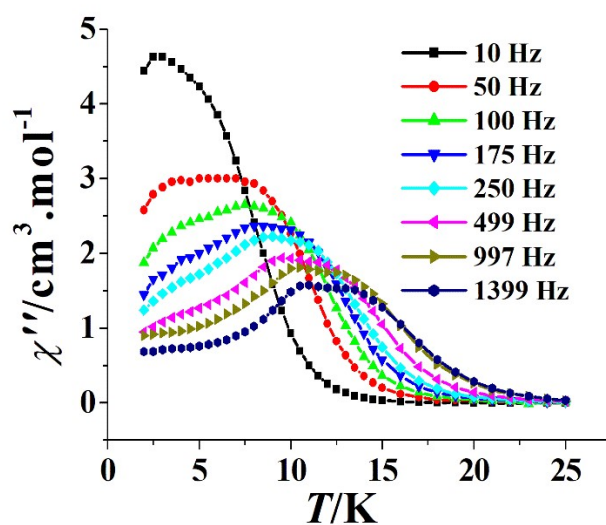


Fig. S5.  $M$  versus  $H$  plots at 2-6 K of 2.

**Table S4.** Linear combination of two modified Debye model fitting parameters from 3 K to 14 K of **1** at 0 Oe dc field.

$T(\text{K})$	$\chi_2(\text{cm}^3 \cdot \text{mol}^{-1})$	$\chi_1(\text{cm}^3 \cdot \text{mol}^{-1})$	$\chi_0(\text{cm}^3 \cdot \text{mol}^{-1})$	$\tau_1(\text{s})$	$\alpha_1$	$\tau_2(\text{s})$	$\alpha_2$
3	25.07181	12.85752	2.32299	0.00527	0.538	0.1675	0.188
4	20.78438	12.20262	1.88733	0.00649	0.518	0.10131	0.174
5	17.73782	8.28603	1.72912	0.0026	0.450	0.0623	0.257
6	15.09536	6.98879	1.59126	0.00182	0.387	0.03563	0.238
7	12.98384	6.422	1.43908	0.00135	0.345	0.02043	0.194
8	11.35637	5.79178	1.29821	0.00088	0.314	0.01126	0.169
9	10.18731	4.65446	1.24507	0.00041	0.251	0.00579	0.173
10	9.17564	4.37171	0.93334	0.00031	0.301	0.00322	0.168
11	8.35459	4.04525	0.99669	0.00022	0.305	0.00181	0.177
12	7.60703	5.31278	1.7959	0.0002	0.258	0.00155	0.116
13	7.02127	5.55415	2.06627	0.00018	0.222	0.00128	0.075
14	6.51789	5.34378	2.31748	0.00012	0.189	0.00094	0.053



**Fig. S6.** Plots of  $\chi''$  versus  $T$  for **1** ( $H_{\text{dc}} = 1500$  Oe).

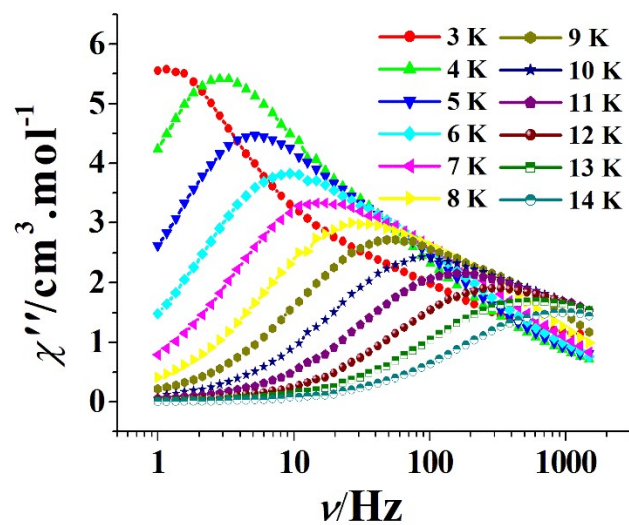


**Fig. S7.** Plots of  $\chi''$  versus  $\nu$  for **1** ( $H_{dc} = 1500$  Oe).

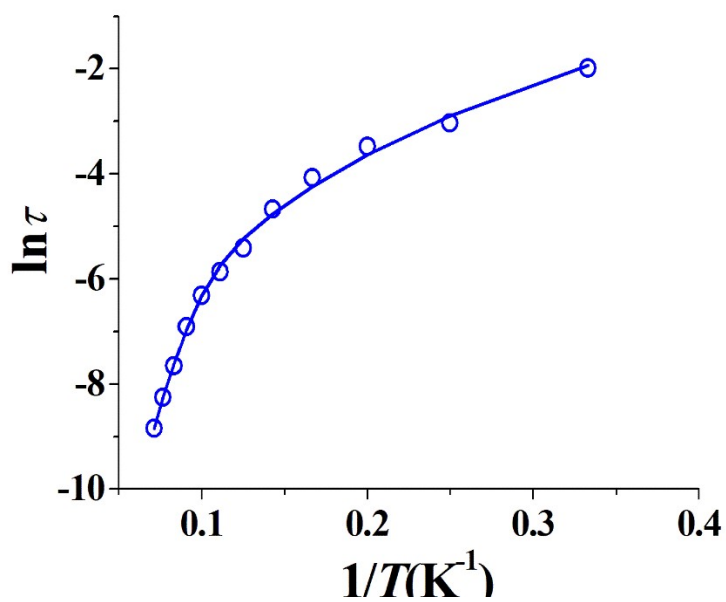


**Fig. S8.** Plot of  $\ln(\tau)$  versus  $1/T$  for **1** ( $H_{dc} = 1500$  Oe); the solid line represents the best fitting with Orbach *plus* Raman.

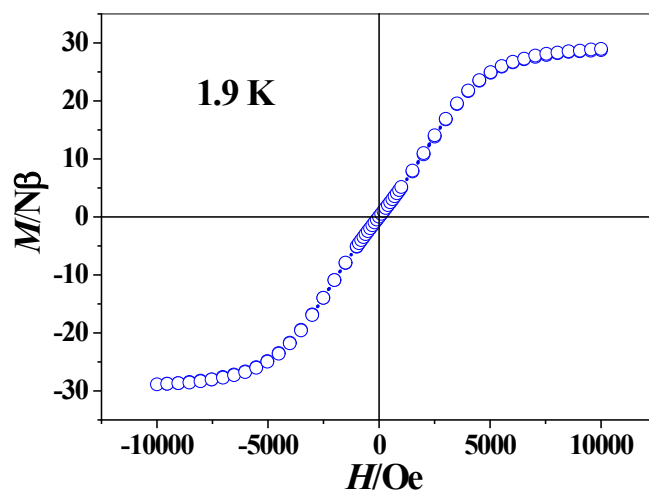


**Fig. S9.** Hysteresis loop for **1** at 1.9 K with the normal sweep rate (100-300 Oe min<sup>-1</sup>).

**Table S5.** Linear combination of two modified Debye model fitting parameters from 4 K to 17 K of **2** at 0 Oe dc field.

$T(K)$	$\chi_2(\text{cm}^3.\text{mol}^{-1})$	$\chi_1(\text{cm}^3.\text{mol}^{-1})$	$\chi_0(\text{cm}^3.\text{mol}^{-1})$	$\tau_1(\text{s})$	$\alpha_1$	$\tau_2(\text{s})$	$\alpha_2$
4	30.41546	26.2716	0.23999	0.10279	0.226	0.00246	0.272
5	26.00194	22.06772	0.20131	0.06227	0.239	0.00205	0.282
6	22.25434	17.6234	0.14548	0.03918	0.227	0.00218	0.319
7	19.19946	14.15368	0.13914	0.02445	0.211	0.00189	0.321
8	16.99774	10.73509	0.1323	0.01623	0.171	0.00182	0.349
9	15.23236	9.86622	0.23595	0.00958	0.172	0.00106	0.344
10	13.78287	9.84581	0.41384	0.00558	0.180	0.00049	0.303
11	12.58207	9.07404	0.54531	0.00343	0.178	0.0003	0.303
12	11.50595	8.00391	0.74549	0.00214	0.161	0.00022	0.313
13	10.63442	7.70631	1.05453	0.00136	0.160	0.00016	0.272
14	9.88637	7.01189	1.4421	0.00091	0.157	0.00015	0.238
15	9.21538	5.47318	1.79264	0.00072	0.139	0.00014	0.193
16	8.63145	5.03484	1.78642	0.00048	0.143	0.00013	0.179
17	8.12767	5.42767	1.86059	0.0003	0.159	0.00007	0.119

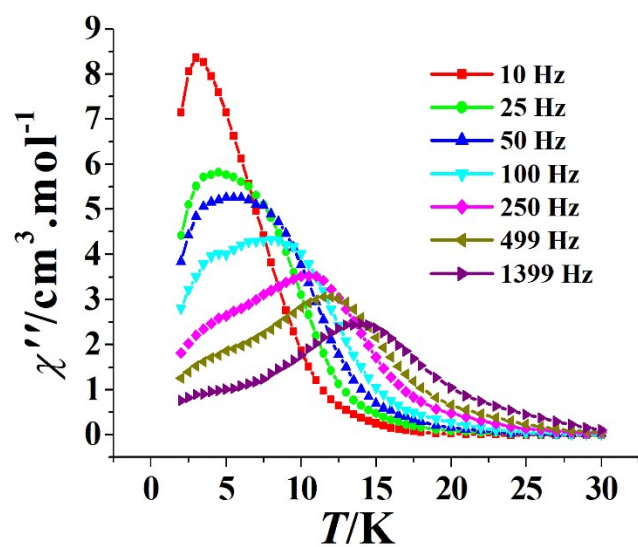


Fig. S10. Plots of  $\chi''$  versus  $T$  for **2** ( $H_{dc} = 1500$  Oe).

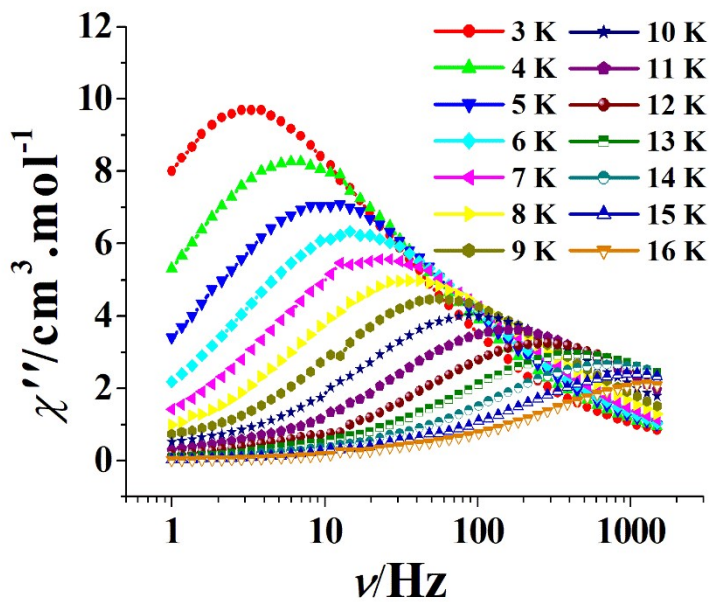
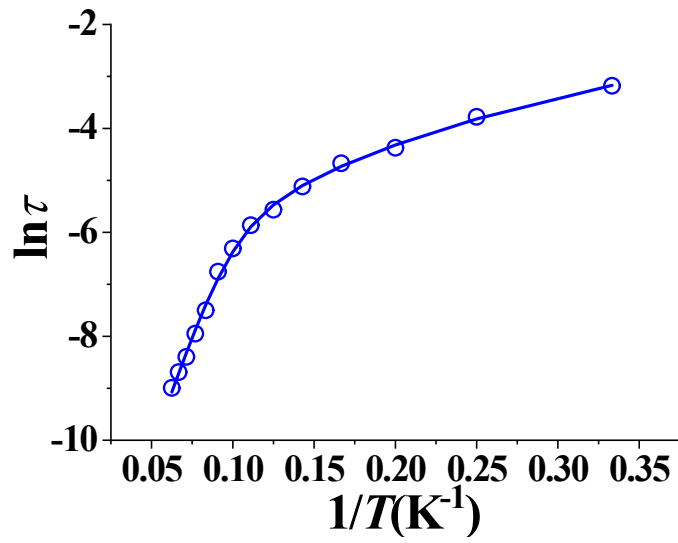
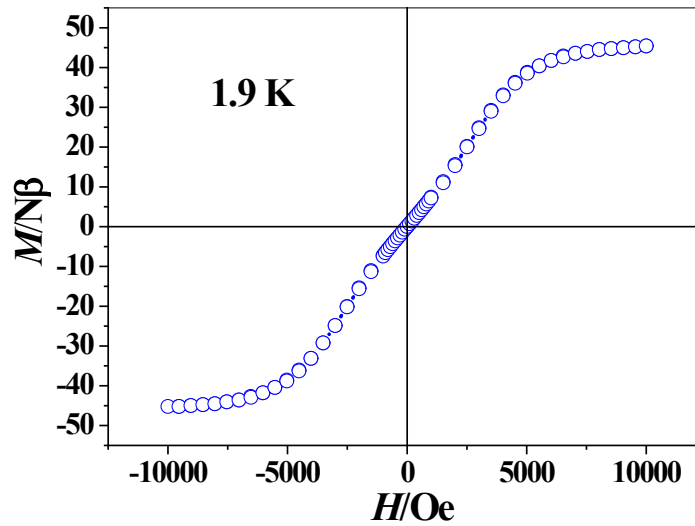


Fig. S11. Plots of  $\chi''$  versus  $\nu$  for **2** ( $H_{dc} = 1500$  Oe).



**Fig. S12.** Plot of  $\ln(\tau)$  versus  $1/T$  for **2** ( $H_{dc} = 1500$  Oe); the solid line represents the best fitting with Orbach *plus* Raman.



**Fig. S13.** Hysteresis loop for **2** at 1.9 K with the normal sweep rate (100-300 Oe  $\text{min}^{-1}$ ).